



High-speed THz spectroscopic imaging at ten kilohertz pixel rate with amplitude and phase contrast

M. BECK,¹ T. PLÖTZING,¹ K. MAUSSANG,² J. PALOMO,² R. COLOMBELLI,³
I. SAGNES,³ J. MANGENEY,¹ J. TIGNON,¹ S. S. DHILLON,² G. KLATT,¹ AND
A. BARTELS,^{1,*}

¹Laser Quantum GmbH, Max-Stromeyer-Str. 116, 78467 Konstanz, Germany

²Laboratoire Pierre Aigrain, Département de physique de l'ENS, École Normale Supérieure, PSL Research University, Université Paris Diderot, Sorbonne Paris Cité, Sorbonne Universités, UPMC Univ. Paris 06, CNRS, 75005 Paris, France

³Centre de Nanosciences et de Nanotechnologies, CNRS, Univ. Paris Sud, Université Paris-Saclay, C2N Marcoussis, 91460 Marcoussis, France

*albrecht.bartels@laserquantum.com

Abstract: By combining the advantages of the high-speed ASOPS technology and efficient THz generation, we have realized a high-speed laser-based spectroscopic THz imaging system with more than 10,000 pixels per second acquisition speed and an excellent signal-to-noise ratio of more than 100. Unlike THz line cameras or mm-wave intensity detectors, the present device allows for a much higher spatial resolution and attributes each imaging pixel with phase and amplitude information up to several THz while simultaneously maintaining a very high scanning speed unmatched by any other technique presented so far. The high-speed acquisition allows for samples to be scanned even at sample velocities of 5 m/s or higher while preserving the fundamental resolution limit of the THz radiation, which is on the order of 500 μm in the present case.

© 2019 Optical Society of America under the terms of the [OSA Open Access Publishing Agreement](#)

1. Introduction

A multitude of different Terahertz spectroscopy techniques have been well established in the past two decades due to inherently interesting properties of the low THz frequency range for applications in fundamental sciences, biological and pharmaceutical industry or security [1–5]. There are numerous advantages when employing THz radiation such as a strong dependence on water content, and the possibility for substance identification since many gases, molecules as well as solid state samples exhibit a unique fingerprint in this frequency range. Particularly interesting are applications where THz radiation is used for imaging since many materials are transparent for THz frequencies such as plastics or paper, in contrast to near-infrared or visible light [4]. Also, THz radiation gives much better spatial resolution compared to microwave-based imaging systems due to the shorter wavelengths employed.

When designing THz imaging devices, the most crucial points are imaging speed, signal-to-noise ratio as well as the type of information that can be interpreted at each pixel such as intensity or spectral amplitude and phase information. The fastest THz devices nowadays are built in the 100 GHz range since the rapid development in thermoelectric cameras enables direct bolometric measurements of CW sources [6] where an image can be formed through beam bending [7] or even 2D cameras for real time imaging [8] so that fast imaging devices can be built. Next generation THz imaging devices are suggested at even higher THz frequencies at specific wavelengths [3]. However, in these measurements light is captured using thermoelectric cameras or an array of microwave antennas so that only the intensity contrast information can be gathered. In addition, the resolution is limited by the limited pixel matrix size of the detection camera and the limited number of antennas in an array or

ultimately by the large wavelength of the radiation employed. Two-dimensional spectroscopic imaging has been demonstrated using electro-optic sampling and a CCD camera, however, these systems typically require amplified lasers with pulse energies in excess of $1\mu\text{J}$ [9].

A common method for THz imaging is based on terahertz time domain spectroscopy. Here THz radiation is generated and detected using ultrafast lasers [2,4,5], permitting a powerful tool that exhibits typically a broad bandwidth up to several THz such that spectroscopic imaging is feasible, as well as amplitude and phase information. At each pixel these devices may gather the full spectral information of a sample with excellent signal-to-noise and high spectral resolution. However, due to the pixel-by-pixel scan technique employed and a mechanical delay line, imaging speed is usually very poor, of the order of 10 pixels per second or less, such that a final image can be acquired only after minutes or even many hours [1,2,5]. THz spectroscopy based on asynchronous optical sampling (ASOPS) overcomes the abovementioned obstacles and provides a unique combination of extreme high data acquisition rates as well as allowing access to amplitude and phase information at the same time for low noise, high precision THz spectroscopy with GHz frequency resolution [10]. Here, the very fast data acquisition rates can be achieved since there is no need for a mechanical delay between the two lasers that is normally required to sample the THz radiation. As is shown here, the presented THz imaging device based on ASOPS is orders of magnitudes faster and more powerful in terms of bandwidth and SNR compared to existing laser-based THz imaging devices [7,8] without the use of THz gratings and calibration of cameras.

2. High-speed ASOPS THz spectrometer

The ASOPS based THz spectroscopy system employed here is based on two high repetition rate lasers running at $f_R = 1$ GHz repetition rate (models *taccor power* from *Laser Quantum*). The lasers are locked together in a master-slave configuration with a slight Δf_R offset between them that can be as high as 20 kHz while maintaining an excellent time resolution [10,11]. The combination of high scan rates and good time resolution can only be achieved with such high repetition rates and is thus a unique feature of the 1 GHz lasers compared to 80 MHz systems where the same physical performance is achieved with scan rates as low as 100 Hz. When $\Delta f_R = 10$ kHz as in the present case, a 1 ns THz waveform can be acquired within only 100 μs of integration time. Figure 1 shows an example measurement of a THz transient and the corresponding Fourier transform. Even without averaging and at these short acquisition times, an excellent signal to noise ratio of more than 100 in the time domain and more than 30 dB in the frequency domain is achieved. Even larger signal to noise (SNR) values can be achieved when using thicker electro-optic detection crystals and when the setup is enclosed and purged with e.g. nitrogen. Note, that the SNR in the frequency domain is usually expressed in terms of spectral power while the time domain is typically related to amplitude information.

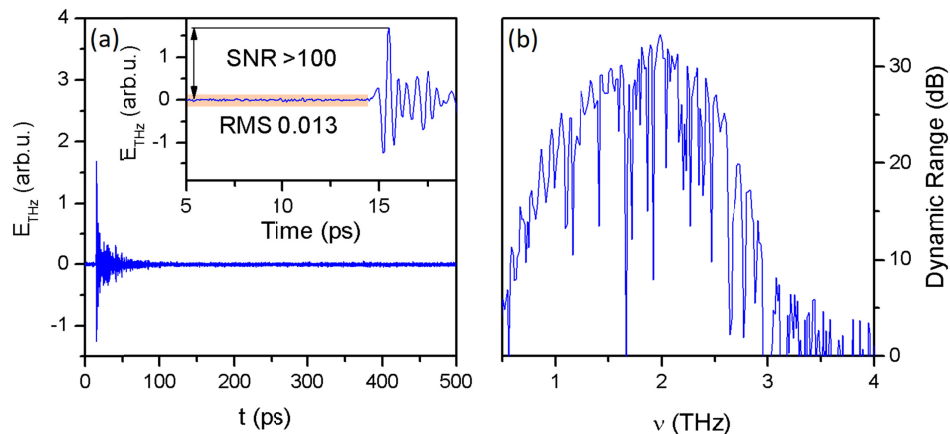


Fig. 1. (a) Single shot of the THz time domain waveform with 500 ps time window. Inset shows a magnification of the time trace indicating a RMS noise value of 0.013 so that the SNR yields more than 100 at 100 μ s measurement time without averaging. (b) Fourier transform of the data shown in (a) indicating more than 30 dB dynamic range in the spectral power.

Since the pulse energy of high repetition rate lasers is in the nJ range, it is crucial to employ highly efficient photoconductive antennas for producing sufficiently large THz electric fields so that averaging is not required. Here, we implement an efficient photoconductive antenna that has been previously reported [12,13], which consists of an interdigitated finger electrode on the surface of a semiconducting material. Just below the surface of the semiconductor there is a metal sheet reflecting a significant portion of the generated THz radiation (i.e. there is no loss THz loss to the substrate). As a consequence, the device collects more THz light. (The device however has to be used in reflection geometry). The increase in efficiency of the device leads to the impressive performance in combination with ASOPS as shown in Fig. 1.

3. Imaging technique

Figure 2(a) shows the schematic of the setup used for imaging. As can be seen, the core layout of the THz time domain spectrometer represents a reflection geometry where the THz beam is guided using off-axis parabolic mirrors (OAP). THz light is emitted using a photoconductive antenna (PCA) and an electro-optic crystal (EOX, a 400 μ m thick (110)-ZnTe crystal) for THz detection. The sample is imaged under a 30 $^\circ$ angle of incidence and resides in the THz focal plane. To acquire a two-dimensional image of the sample it is scanned in two axes. Instead of moving the sample along Cartesian coordinates, here, we employ a different approach as can be seen in Fig. 2(b). The sample is moved in one direction using a translation stage at a speed v and simultaneously rotated at speed ω . The axes are chosen such that, both, rotational movement as well as the translational movement keep the sample in the focal plane of the THz beam. When continuously acquiring THz data while rotating and moving the sample as discussed, the sample is scanned along a spiral curve as shown in Fig. 2(c). The green circles indicate the measured pixels N_i . When carefully choosing the values for v and ω , it can be achieved that spatial separation Δx of the pixel N_i and N_T along the translational movement axis is less than the spatial resolution of the device, in the present case smaller than 500 μ m. N_T describes the pixel number after one full rotation has been performed with duration $T = 1/\omega$. The time between two adjacent pixels, e.g. N_1 and N_2 , is equal to the measurement acquisition time of the current device which in the present case is 100 μ s.

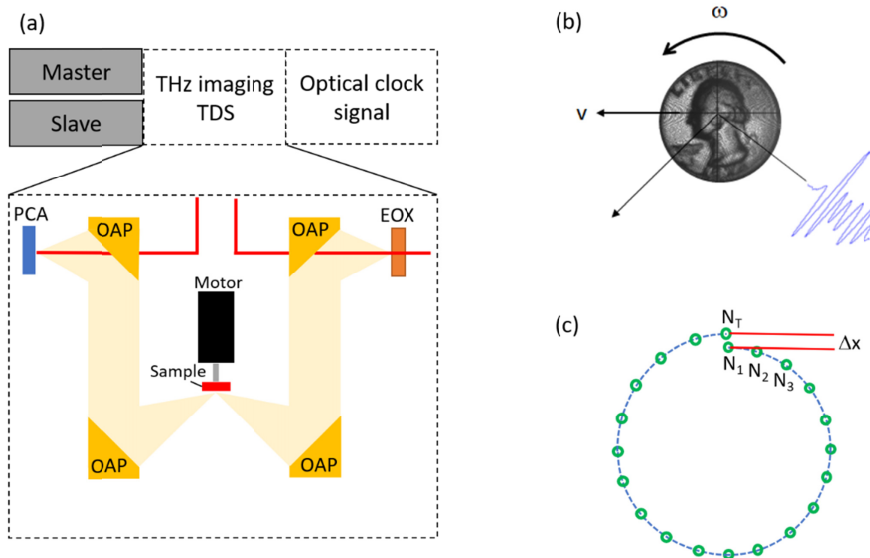


Fig. 2. (a) Reflection measurement geometry of the sample under investigation. (b) The sample is rotated at the speed ω , while it is simultaneously being translated at constant speed v . In this layout the THz focus is fixed in space so that the sample is scanned in a spiral movement (c).

Since the acquisition time is so short, an FPGA based data acquisition card from *Gage Appl. Inc.* is employed to store the handle the measured information. The card can store several Gigabit of data in onboard memory for further data management, thus enabling such high acquisition rates. The onboard memory is sufficient for the current experiment. In cases where the onboard memory is not enough, the card supports data streaming to continuously write the measured data to a hard drive.

Since the sample is continuously in motion the pixel position is imprinted as a function of time. In order to assign the measured THz transient N_i to the according pixel position, we need to keep track of two sets of trigger signals. Simultaneously to the THz signal, there is an optical clock signal that is generated by the two lasers via a cross-correlation in a two-photon absorption diode. As can be seen in Fig. 3, the optical clock signal arrives simultaneously to the THz signal (as they originate from the same sources). The separation between two THz traces is $\tau = 1/\Delta f_R$ which in our case is 100 μs . By triggering the data acquisition card to this signal, each THz waveform can be collected and labeled due to the precise time base of the data acquisition card. Within the time frame of one rotation of the sample, there are hundreds or few thousands of measurements N_i depending on the ratio $\Delta f_R/\omega$. In addition, a light barrier sensor on the rotation motor indicates completion of a full revolution after time T , helping to account for slight variations in rotation speed during image acquisition when re-constructing the image. The advantage of the rotational approach is the high possible scanning speed permitting interpixel separation at the optical resolution limit. Employing the ASOPS principle is key to enabling this technique. THz spectroscopic imaging with spectral coverage around 1 THz is typically limited to a spatial resolution of approximately 500 μm per pixel due to fundamental wave limits if no near-field techniques are employed. In combination with the presented high-speed THz spectrometer it is thus possible to scan a sample even when it is moving as fast as 5 m/s or faster while maintaining the fundamental pixel resolution. This speed has so far only been shown with 100 GHz line scan technique where the spatial resolution is of order 3 mm and the image is formed solely by intensity contrast [3].

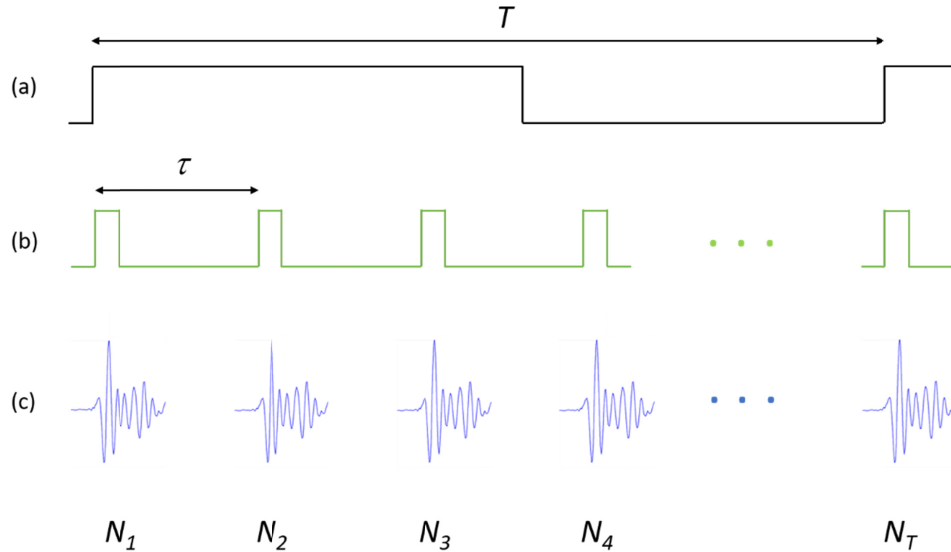


Fig. 3. Timing and Reference Signals in relation to the THz waveform signals. (a) Clock signal that counts the round trips of the coin. (b) Optical clock signal used to trigger the data acquisition card. The optical clock signal temporally coincides with each THz transient (c).

4. Data analysis

To demonstrate the capabilities of the system, high speed imaging of a metal coin is shown. The coin has a diameter of 2.4 cm and exhibits thin line features as well as an overall height distribution. The rotation speed is chosen to be $\omega = 10$ Hz so that within $T = 100$ ms approximately 1000 waveforms are acquired during one full rotation of the sample. The translational movement of the coin is $v = 1.5$ mm/s. While the sample is moving and spinning, the THz spectrometer continuously acquires data. The values for ω and v have been chosen carefully to avoid aliasing and under-sampling of the final image. The complete coin can be acquired within only 13 seconds, while a conventional non-ASOPS setup would require many hours to achieve a result similar in spatial and spectral resolution. The result is shown in Fig. 4 next to a photograph of the coin. The final THz image on the left side consists of approximately 130 000 pixels with a 500 μm spatial resolution. Each pixel contains amplitude and phase information of the measurement. Note, that the spatial resolution is limited by the THz fundamental properties and not by measurement speed of the system. The nominal pixel size is less than 100 μm . Each measured THz transient can be related to the pixel position since a light barrier signal monitoring rotational speed and angle position of the coin is simultaneously recorded, thus keeping the position error much smaller than the spatial resolution.

The pixel information in the image shown represents the spectral intensity integrated between 2 and 3 THz to enhance the image contrast of the smaller features. Post processing of the measured was done after the measurement but could in principle be calculated simultaneously to the measurement of the data, assuming that the PC used has the computational power to handle the calculations while streaming the data from the measurement card to the hard drive. The intensity contrast in the image originates from the coin geometry. However, images from a sample showing spectroscopic contrast could be obtained in a straightforward manner although the measurement speed may have to be reduced for weak spectroscopic features. The spectroscopy capabilities of the ASOPS based THz technique have been outlined in more detail in [14].

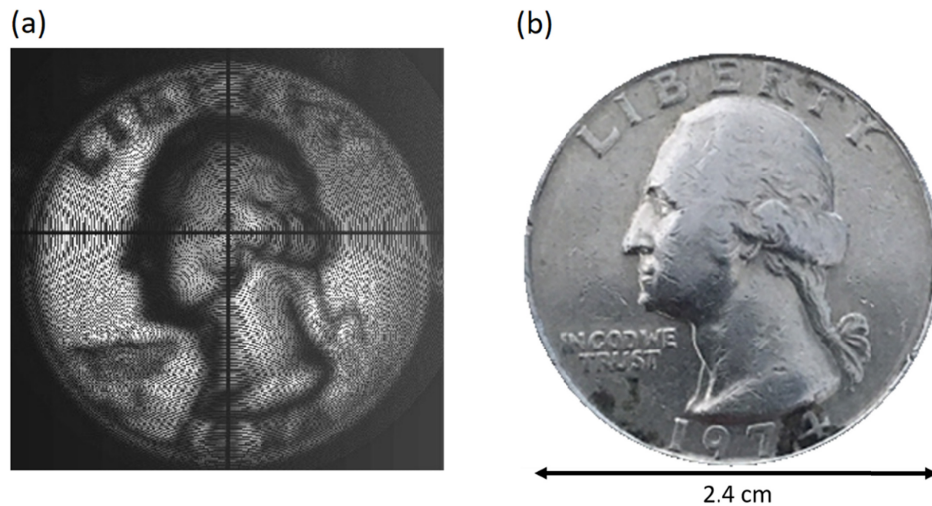


Fig. 4. (a) Final THz contrast image consisting of 130 000 pixels measured within 13s. Each pixel contains the spectral intensity integrated between 2 and 3 THz. (b) Photograph of the coin for comparison.

5. Summary

Combining the advantages of high-speed ASOPS technology and efficient, modern THz antennas we created a cutting-edge powerful spectroscopic THz imaging system that is capable of recording more than 10,000 pixels per second, with an excellent signal to noise ratio of more than 100 (in the time-domain data). Unlike THz line cameras or mm-wave intensity detectors, the present device even allows for a much higher spatial resolution and attributes each imaging pixel with phase and amplitude information. The high-speed data imaging allows for samples to be scanned at velocities 5 m/s or higher while preserving the fundamental limit of the THz radiation which is on the order of 500 μm in the present case. As an example, a 2.4 cm diameter metal coin has been imaged in only 13 seconds for a THz image consisting of 130 000 pixels.

References

1. Y. Garini, I. T. Young, and G. McNamara, "Spectral imaging: principles and applications," *Cytometry A* **69**(8), 735–747 (2006).
2. B. B. Hu and M. C. Nuss, "Imaging with terahertz waves," *Opt. Lett.* **20**(16), 1716–1718 (1995).
3. B. N. Behnken, G. Karunasiri, D. R. Chamberlin, P. R. Robrish, and J. Faist, "Real-time imaging using a 2.8 THz quantum cascade laser and uncooled infrared microbolometer camera," *Opt. Lett.* **33**(5), 440–442 (2008).
4. S. S. Dhillon, M. S. Vitiello, E. H. Linfield, A. G. Davies, M. C. Hoffmann, J. Booske, C. Paoloni, M. Gensch, P. Weightman, G. P. Williams, E. Castro-Camus, D. R. S. Cumming, F. Simoens, I. Escorcia-Carranza, J. Grant, S. Lucyszyn, M. Kuwata-Gonokami, K. Konishi, M. Koch, C. A. Schmuttenmaer, T. L. Cocker, R. Huber, A. G. Markelz, Z. D. Taylor, V. P. Wallace, J. A. Zeitler, J. Sibik, T. M. Korter, B. Ellison, S. Rea, P. Goldsmith, K. B. Cooper, R. Appleby, D. Pardo, P. G. Huggard, V. Krozer, H. Shams, M. Fice, C. Renaud, A. Seeds, A. Stöhr, M. Naffaly, N. Ridler, R. Clarke, J. E. Cunningham, and M. B. Johnston, "The 2017 terahertz science and technology roadmap," *J. Phys. D Appl. Phys.* **50**(4), 043001 (2017).
5. D. M. Mittleman, "Twenty years of terahertz imaging [Invited]," *Opt. Express* **26**(8), 9417–9431 (2018).
6. G. Ok, K. Park, H. J. Kim, H. S. Chun, and S.-W. Choi, "High-speed terahertz imaging toward food quality inspection," *Appl. Opt.* **53**(7), 1406–1412 (2014).
7. D.-S. Yee, K. H. Jin, J. S. Yahng, H.-S. Yang, C. Y. Kim, and J. C. Ye, "High-speed terahertz reflection three-dimensional imaging using beam steering," *Opt. Express* **23**(4), 5027–5034 (2015).
8. N. Kanda, K. Konishi, N. Nemoto, K. Midorikawa, and M. Kuwata-Gonokami, "Real-time broadband terahertz spectroscopic imaging by using a high-sensitivity terahertz camera," *Sci. Rep.* **7**(1), 42540 (2017).
9. Z. Jiang and X.-C. Zhang, "Terahertz Imaging via Electrooptic Effect," *IEEE Trans. Microw. Theory Tech.* **47**(12), 2644–2650 (1999).
10. G. Klatt, R. Gebbs, C. Janke, T. Dekorsy, and A. Bartels, "Rapid-scanning terahertz precision spectrometer with more than 6 THz spectral coverage," *Opt. Express* **17**(25), 22847–22854 (2009).

11. R. Gebs, G. Klatt, C. Janke, T. Dekorsy, and A. Bartels, "High-speed asynchronous optical sampling with sub-50fs time resolution," *Opt. Express* **18**(6), 5974–5983 (2010).
12. K. Maussang, J. Palomo, J.-M. Manceau, R. Colombelli, I. Sagnes, L. H. Li, E. H. Linfield, A. G. Davies, J. Mangeney, J. Tignon, and S. S. Dhillon, "Monolithic echo-less photoconductive switches as a high-resolution detector for terahertz time-domain spectroscopy," *Appl. Phys. Lett.* **110**(14), 141102 (2017).
13. K. Maussang, A. Brewer, J. Palomo, J.-M. Manceau, R. Colombelli, I. Sagnes, J. Mangeney, J. Tignon, and S. S. Dhillon, "Echo-Less Photoconductive Antenna Sources for High-Resolution Terahertz Time-Domain Spectroscopy," *IEEE Trans. Terahertz Sci. Technol.* **6**(1), 20–25 (2016).
14. G. Klatt, R. Gebs, H. Schäfer, M. Nagel, C. Janke, A. Bartels, and T. Dekorsy, "High-Resolution Terahertz Spectrometer," *IEEE J. Sel. Top. Quantum Electron.* **17**(1), 159–168 (2011).